Exp Brain Res
DOI 10.1007/s00221-006-0652-y

RESEARCH ARTICLE

Deciding when and how to correct a movement: discrete submovements as a decision making process

Alon Fishbach · Stephane A. Roy · Christina Bastianen · Lee E. Miller · James C. Houk

Received: 10 November 2005 / Accepted: 24 July 2006

Abstract Rapid reaching movements of human and non-human primates are often characterized by irregular multi-peaked velocity profiles. How to interpret these irregularities is still under debate. While some reports assert that these irregularities are the result of a continuous controller interacting with the environment, we and others hold that the velocity irregularities are evidence for a controller that produces discrete movement corrections. Here we analyze rapid pronation/supination wrist movements in monkey during a 1D step-tracking task, where visual perturbations of the target were randomly introduced at movement onset. We use our recently introduced algorithm (Fishbach et al. in Exp Brain Res 164:442–457, 2005) to decompose an irregular movement into a primary movement and one or more discrete, corrective submovements. We first show that the visual perturbation has almost no effect on primary movements. In contrast, this perturbation influences the type and the extent of the corrective submovements that often follow primary movements. Secondly, we show that the highly variable *timing* of overlapping submovements does not depend directly on the visual perturbation but rather on an estimate of the movement error and on the movement's extent-to-go at the time of correction initiation. These results are consistent with a forward-model based intermittent controller with a non-linearity that depends both on a prediction of the magnitude and direction of the movement's error and on its *variance*. Corrections are initiated only when the predicted error is statistically significant. A simple abstract model that implements these principles accounts for the type and timing of the corrections observed in our data.

Keywords Intermittent control · Forward model · Decision making · Error correction · Submovements · Monkey

A. Fishbach (✉)
Department of Physical Medicine and Rehabilitation,
Northwestern University, 345 E. Superior St., Room 1436c,
Chicago, IL 60611, USA
e-mail: fishbach@northwestern.edu

A. Fishbach
SMPP, Rehabilitation Institute of Chicago,
345 E. Superior St., Room 1436c,
Chicago, IL 60611, USA

S. A. Roy · C. Bastianen · L. E. Miller · J. C. Houk
Department of Physiology, Northwestern University,
303 East Chicago Ave., Chicago, IL 60611, USA

S. A. Roy · C. Bastianen
Department of Neurology, Evanston Hospital,
Evanston, IL 60201, USA

Introduction

Reaching movements of primates under constraints of time and spatial accuracy are often characterized by irregular and asymmetric multi-peaked velocity profiles (Milner and Ijaz 1990; Novak et al. 2000, 2002; Fishbach et al. 2005). Despite the abundant experimental evidence for these kinematic irregularities, their interpretation remains controversial. While many studies have interpreted these irregularities as evidence for the superposition of multiple overlapping movement primitives (Woodworth 1899; Morasso and Mussa Ivaldi 1982; Meyer et al. 1988; Flash and Henis 1991; Milner 1992; Pratt et al. 1994; Berthier 1996; Lee

et al. 1997; Novak et al. 2000, 2002; Fishbach et al. 2005), others have interpreted them as the outcome of a continuous control process interacting with the environment (Kawato 1992; Shadmehr and Mussa-Ivaldi 1994; Bhushan and Shadmehr 1999).

Recently we introduced a novel ''soft-symmetry'' method for analyzing irregular movements and decomposing them into their discrete movement primitives, namely a primary movement followed by one or more overlapping submovements (OSMs) (Fishbach et al. 2005). In that paper, the kinematics of rapid pronation/supination wrist movements in monkeys performing a 1D step-tracking task were analyzed using that method. The kinematic properties of both primary regular movements (ones that lacked OSMs) and delayed submovements (DSMs, corrections that did not overlap the primary movement but rather started after the primary movement ended) were compared with the properties of movement primitives that were extracted from irregular movements. We demonstrated that several properties of the extracted submovements were very similar to those of regular movements, thus supporting the hypothesis that movement irregularities result from the superposition of discrete movement primitives.

In the present study, we further evaluate the interpretation of kinematic irregularities as the superposition of discrete movement primitives and contrast it with the alternative hypothesis that the irregularities are the result of a continuous controller. For this purpose, we analyze the corrective submovements of two monkeys performing a 1D tracking task where the target was occasionally visually perturbed at movement onset. We examine the effect of the visual perturbation on the kinematic properties of both the primary movement and the corrective submovements. In particular, we examine the timing and the conditions under which the motor system uses overlapping and delayed submovements both in the perturbed and in the unperturbed conditions. If the kinematic irregularities were the outcome of a continuous controller, we would expect that the visual perturbation would trigger a smooth or an abrupt correction to compensate for the new location of the target. If a continuous controller were to use visual feedback throughout the movement, the correction initiation time should be of a relatively fixed latency across trials; a latency corresponding to the sensorimotor delay (Saunders and Knill 2003). A second possibility is that a continuous controller might use visual information only at the end-phase of the movement. In this case the correction initiation time would depend on the cursor location relative to the target just before the correction initiation.

Our results support neither of these possibilities. We show that the visual perturbation has almost no effect on the primary movement's shape or amplitude, thus ruling out a smooth continuous update during the initial part of the movement. The change in the movement's total extent due to the visual perturbation is carried out by altering the number and extent of discrete submovements. Despite this significant effect, the visual perturbation had almost no effect on the timing of these corrections, which was mainly correlated with the expected error of the ongoing movement and with the movement's expected extent-to-go at the time of correction initiation.

These results are consistent with a forward-model intermittent controller with a non-linearity that depends both on a prediction of the movement error and on the estimated *variance* of the predicted error. Thus a correction is not necessarily initiated when the expected error crosses a threshold (Hanneton et al. 1997); instead, a decision to correct is made when the *probability distribution* of the predicted end-point is statistically different from the target's location. We show that a simple abstract model that implements these principles can account for the type and timing of the corrections observed in our data.

Materials and methods

Experimental setup

The details of the experimental setup were described elsewhere (Fishbach et al. 2005). In short, two macaque monkeys (monkey V.—male *Macaca mullatta* and monkey L.—female *Macaca fascicularis*) were trained to perform a one-dimensional step-tracking task. Monkeys sat in a monkey chair facing a 14″ computer monitor and gripped a low friction rotating handle that controlled the horizontal position of a round cursor on the screen in response to supination/pronation movements of the forearm. The handle was equipped with a potentiometer and a low-noise tachometer that measured the position and angular velocity of the handle, respectively. The position and velocity signals were measured with a resolution of 0.1683° and 2.2 deg/s, respectively, and sampled at a rate of 1,000 Hz for storage and analysis. Digital filtering and analysis were performed using Matlab (The MathWorks). Velocity and its derivatives were filtered with a 35 ms Hanning window. The filtered velocity had a noise RMS level of 0.51 deg/s; the acceleration, jerk and snap had noise RMS levels of 0.036 Kdeg/s^2, 0.0057 Mdeg/s^3 and 1.76 Mdeg/s^4, respectively. At the beginning of a block

of trials, a starting target in the shape of a box was illuminated on the screen at a random position out of three possible target positions (left, center or right). After the cursor was moved to the starting location, a second target that was randomly chosen out of the two remaining locations was illuminated, and the starting target turned off (Fig. 1). The monkey had unlimited time to respond but once moving the cursor the monkey had to reach the second target within 500 ms. The three target positions (left, center and right) corresponded to rotations of the handle of –45, 0, 45°, respectively and the target's width extended over an equivalent of a 12° of handle rotation. On two-thirds of the trials the target was visually perturbed by a distance that was equivalent to 7.2° and 14.4° of the handle rotation for the 45° and 90° trials, respectively. The target perturbation occured at movement onset, when the cursor first left the starting location, either toward the cursor location (''near perturbation'') or away from the cursor (''far perturbation''). The unperturbed, near perturbed and far perturbed conditions were randomly allocated across the trials. Visual perturbations were introduced and data were collected after the monkeys were trained with no visual perturbations and were performing the task accurately and within the time constraints on 80% of the trials. All procedures were approved by the Institutional Animal Care and Use Committee of Northwestern University and adhere to the National Institutes of Health Guide for the Care and Use of Laboratory Animals.

Data analysis

Angular velocity profiles were analyzed using the 'soft-symmetry' method we have recently introduced (Fishbach et al. 2005). In short, for each trial, the onset and offset times of non-overlapping movement primitives were defined using two fixed thresholds of the velocity, θ_1 and θ_2, which were set to five and 34 deg/s, respectively. The onset time, T_{on} was defined as the last time the velocity increased past θ_1 before reaching θ_2. The movement offset time was analogously defined as the first time the velocity reached θ_1 after decreasing below θ_2. The use of two thresholds instead of one offers more tolerance to noise and to the choice of threshold values.

Occurrence of overlapping submovements was identified by examining the higher time derivatives of the velocity trace. A regular primary movement, which

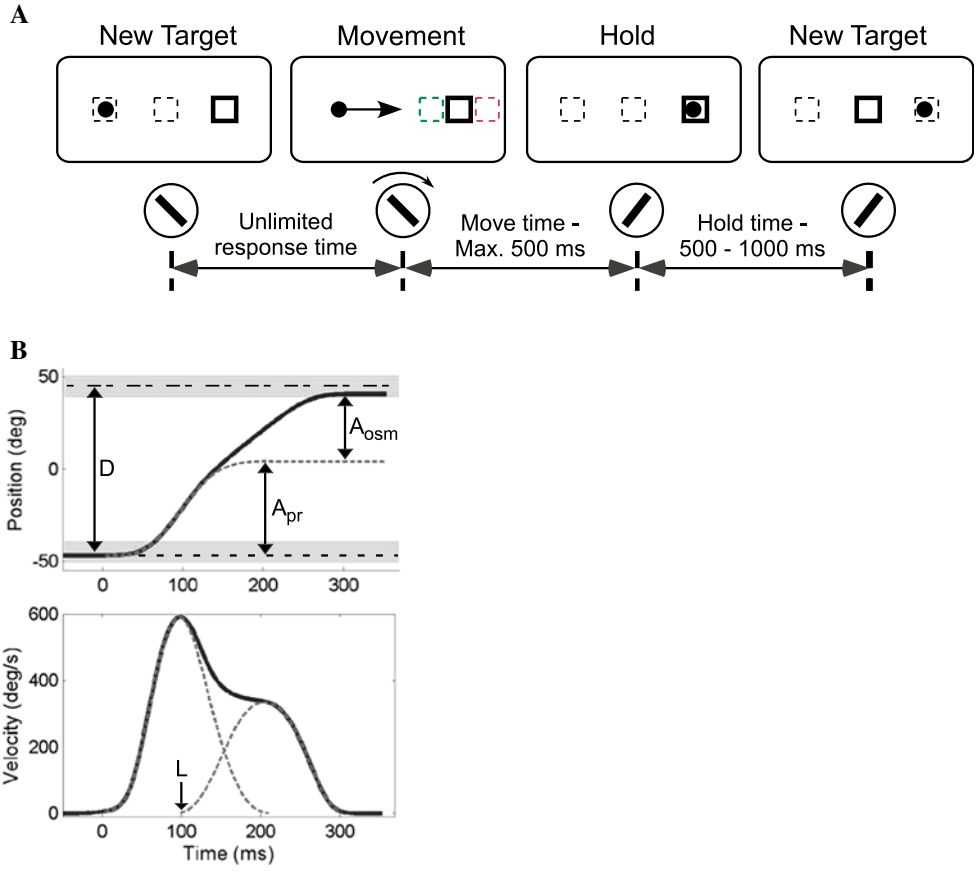

Fig. 1 **a** Schematic diagram of experimental setup. See more details in text. **b** Position (*upper panel*) and velocity (*lower panel*) as a function of time for a typical irregular movement that was decomposed to a primary movement and an overlapping submovement. A_{pr} denotes that extent of the primary movement, calculated in this case by integrating the primary velocity trace. A_{OSM} and L denote the amplitude and latency of the overlapping submovement, respectively. D is the distance of the cursor from the target at movement onset

is not followed by an OSM, was characterized by exactly two inflection points that corresponded to a pair of jerk zero-crossings or a pair of extrema points in the acceleration, and snap of the movement. Each additional pair of inflection points is being interpreted as an evidence for the existence of a movement primitive, which overlaps the previous movement primitive. The primary movement and corrective submovements were extracted from the combined velocity trace using a monotonic parametric transition function, $R(t)$, which quantifies the percentage of the combined velocity trace that is being contributed by the correction at each point of time. In order to reduce the search space for the optimal $R(t)$, we approximate it using the following functional form:

$$R(t) = \frac{\mathrm{erf}((t-\tau)/\sigma)+1}{2} \quad \text{where } \mathrm{erf}(x) = \frac{2}{\sqrt{\pi}}\int_0^x \mathrm{e}^{-y^2}\mathrm{d}y.$$

The parameters of the transition function (σ and τ, which vary the steepness and mid-point of $R(t)$, respectively) were chosen to maximize the symmetry of the primary movement while keeping the total number of inflection points identical to the number that was observed in the combined velocity trace (for more details see Fishbach et al. 2005).

In order to quantify the symmetry of the angular velocity profile of regular primary movements we use the symmetry index we have introduced before (Fishbach et al. 2005):

$$S = \frac{\sum_{i=1}^{T_v-1}(V(T_v-i)) - \sum_{i=1}^{T_v-1}(V(T_v+i))}{\sum_{i=1}^{T_v-1}(V(T_v-i)+V(T_v+i))},$$

where V is the angular velocity and T_v is the time of peak velocity. If the duration of V is not equal to $2T_v$–1, V is padded with zeros as required. The symmetry index S measures the difference between the movement displacement before and after the time of peak velocity normalized by the total movement displacement. Symmetric movements have an $S = 0$, while movements with larger acceleration than deceleration displacement have an $S > 0$.

The normalized amplitude of primary movements and delayed submovements was defined as the amplitude of the movement over the distance to the target's center before the primary movement or delayed submovement had started. Using the notation of Fig. 1b normalized movement amplitude is calculated as follows:

$$\hat{A} = \frac{A_{\mathrm{pr}}}{D}.$$

The normalized amplitude of an OSM was defined as the amplitude of the OSM over the distance to the target had the OSM not been executed. In the notation of Fig. 1b, the normalized OSM amplitude is calculated as follows:

$$\hat{A}_{\mathrm{OSM}} = \frac{A_{\mathrm{OSM}}}{D - A_{\mathrm{pr}}}.$$

The percent extent-to-go of a movement primitive was defined as:

$$X(t) = 1 - \frac{\sum_i^t V(i)}{\sum_i^n V(i)},$$

where n is the movement duration.

The latency of a submovement was defined as the time interval between the primary movement onset time and the submovement onset time (Fig. 1b). Sensitivity analysis of submovement latency showed a 95% confidence interval of 20 ms (Fishbach et al. 2005).

Results

Both monkeys made rapid pronation/supination movements to align a cursor to a 12° wide target that was 45° or 90° away (Fig. 1a). Often the target was not acquired with a single primary movement, and one or more additional submovements were added to acquire the target. The velocity trace of each trial was decomposed into a primary movement and zero or more submovements as described in detail elsewhere (Fishbach et al. 2005). A submovement that did not overlap its preceding movement primitive was termed a delayed submovement (DSM), and a submovement that overlapped its preceding movement primitive was termed an overlapping submovement (OSM). A total of 7,184 trials from monkey L and 2,649 trials from monkey V were analyzed and were decomposed to 17,115 movement primitives for monkey L. and 8211 movement primitives for monkey V. Figure 2 shows the distribution of the number of movement primitives per trial for each perturbation condition (near, far and no perturbation). The visual perturbation had a marked effect on the number of primitives used in each trial. Near perturbations caused both monkeys to use fewer submovements than they used when no perturbations were introduced. More submovements were used under the far perturbation than under the no perturbation condition.

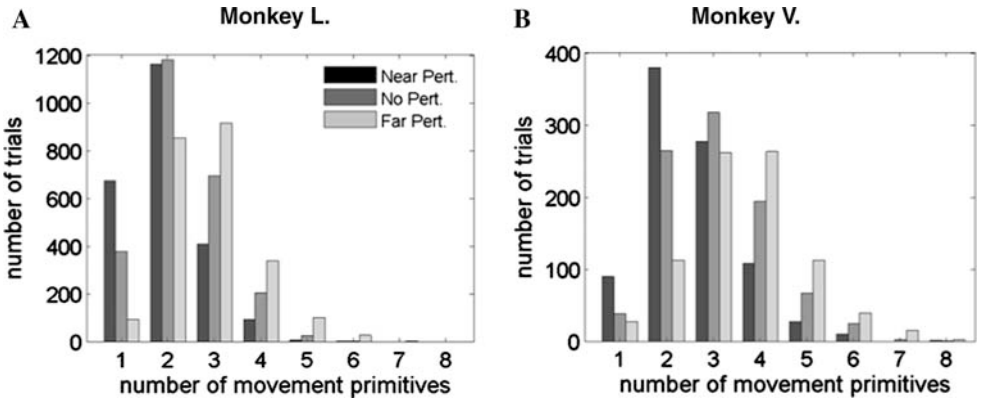

Fig. 2 Distribution of the number of movement primitives per trial per each perturbation condition (near, far and no perturbation) for Monkey L. (**a**) and V. (**b**). Fewer primitives are needed to obtain the target under near perturbations while more primitive are needed under far perturbations

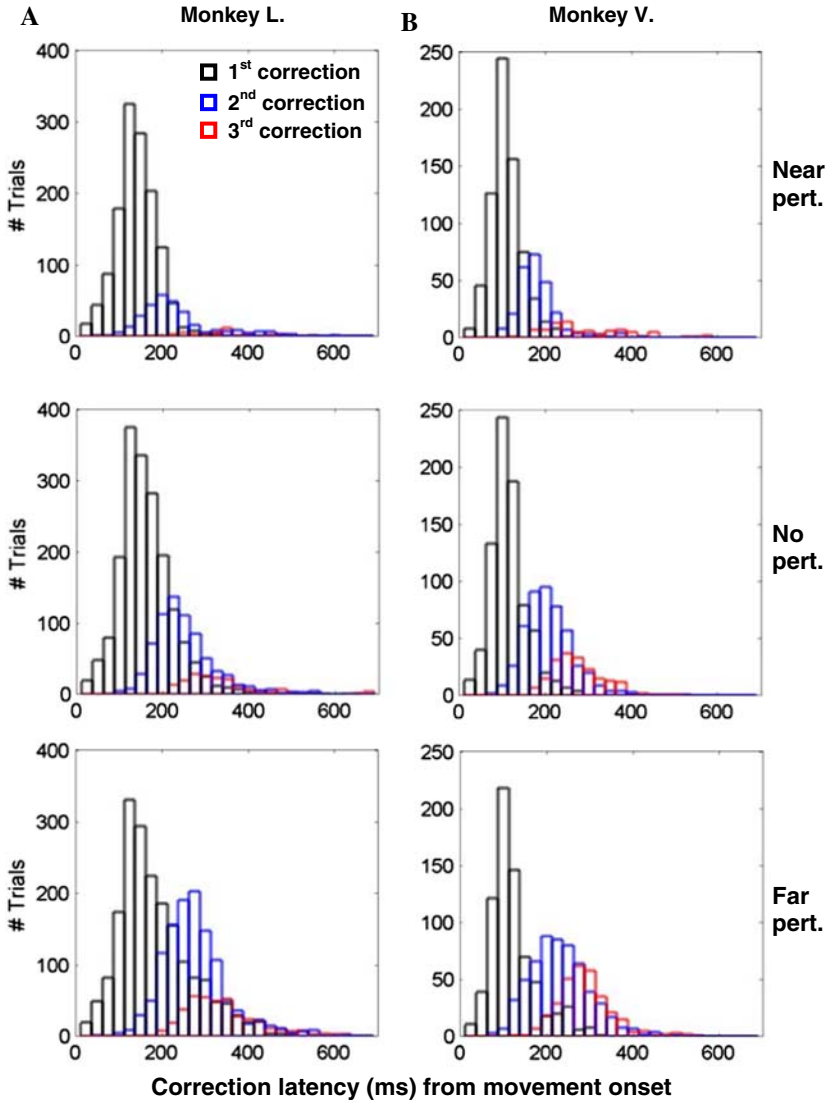

Fig. 3 Distribution of correction initiation times for the first three corrections per perturbation condition. The effect of the visual perturbation is not locked to a specific time but is spread over a time window of more than 200 ms starting at 180 ms after movement onset

Figure 3 plots the distribution of correction initiation times (latencies) relative to movement onset for the two monkeys. This plot highlights three important observations regarding the correction latencies. First, the timing of corrections was highly variable in all perturbation conditions. Second, a considerable number of corrections were initiated very early, in less than 100 ms, after movement onset. Third, the effect of the

visual perturbation on the number of corrections was not locked to a fixed time relative to movement (and perturbation) onset. Rather, the effects of visual perturbation start appearing after about 200 ms and spread throughout the movement duration.

In the following we analyze in detail the effects of the visual perturbation on the size and shape of the primary movements and on the type, timing and size of the ensuing corrective submovements.

Effects of perturbation on primary movements

Normalized movement amplitude

For the analysis of perturbation effects on the amplitude of primary movements, we include both regular primary movements and primary movements that were extracted from irregular movements. Normalized amplitude was analyzed with respect to the type of perturbation (none, near and far perturbation) and with respect to the start to end target extent (45°, 90°). The means and standard deviations of these movement amplitudes for both monkeys are presented in Table 1. A two-factor analysis of variance showed a significant main effect for the start to end target extent factor; the normalized amplitude for 90° trials was smaller than the normalized amplitude for 45° trials (monkey L. $F_{(1,7038)} = 1128.4$, $P < 0.05$; monkey V. $F_{(1,2575)} = 65.4$, $P < 0.05$). There was no significant effect caused by the perturbation factor (monkey L. $F_{(2,7038)} = 0.14$, $P > 0.05$; monkey V. $F_{(2,2575)} = 1.12$, $P > 0.05$) and no significant interaction between the perturbation type and the start-end target extent (monkey L. $F_{(2,7038)} = 0.2$, $P > 0.05$; monkey V. $F_{(2,2575)} = 0.05$, $P > 0.05$). Analyzing regular primary movements and primary movements that were extracted from irregular movements separately show similar results with the exception that the effect of the start to end target extent factor in money V. was not statistically significant, probably because of the small number of cases.

Because of the visual feedback delay we examined the possibility that the effect of visual perturbation on normalized amplitude is significant only for primary movements of long enough duration. For this purpose we sorted the primary movements of each monkey in ascending duration and divided them to ten equal size groups. Analysis of the effect of perturbation on primary movement normalized amplitude that was carried out separately for each group did not find a time window for which the perturbation effect on amplitude was significant (for both L. and V.).

The normalized amplitude takes into consideration the entire movement and therefore might mask out movement updates that occur during the later stages of the primary movement. In order to examine this possibility more precisely we compared the relative movement extent before peak velocity and after peak velocity using the symmetry index. Since the algorithm for the extraction of primary movements from irregular movements tends to create symmetric movements (Fishbach et al. 2005), we used only regular primary movements for this analysis.

The symmetry of regular primary movements was analyzed with respect to the type of perturbation and with respect to the trial extent. The mean and standard deviation values of the movement symmetry for both monkeys are presented in Table 2. A two-factor analysis of variance showed different results for the two monkeys. For monkey L. the main effect for the trial extent factor was not significant ($F_{(1,1947)} = 1.6$, $P > 0.05$) but the main effect for the perturbation factor was statistically significant ($F_{(2,1947)} = 21{,}8$, $P < 0.05$). Surprisingly, regular primary movements tend to have more negative symmetry index (S) under the near perturbation than under far perturbation or no perturbation trials (Table 2). This finding suggests that monkey L., when faced with near perturbations, tended to slightly extend the decelerating part of the primary movement in a way which was not detected by our corrective movement detection algorithm. The interaction analysis showed that this effect was significantly larger for the 90° target pairs than for 45° target pairs ($F_{(2,1947)} = 8.9$, $P < 0.05$). However, the size of the perturbation effect on symmetry was small; the average total increase in movement extent under the near perturbation condition was 1.6% for the 45° trials and 5.1% for the 90° trials. For monkey V. both main effects and the interaction were non-significant (trial extent factor, $F_{(1,220)} = 0.36$, $P > 0.05$; perturbation factor, $F_{(2,220)} = 0.55$, $P > 0.05$; interaction, $F_{(2,220)} = 1.27$, $P > 0.05$).

Table 1 Normalized amplitude of primary movements as a function of start-end target pair and perturbation type

Subject	Start-end target pair	No perturbation	Near perturbation	Far perturbation
L.	45°	0.725 ± 0.201	0.727 ± 0.192	0.726 ± 0.207
	90°	0.557 ± 0.191	0.556 ± 0.19	0.563 ± 0.191
V.	45°	0.608 ± 0.189	0.615 ± 0.21	0.638 ± 0.649
	90°	0.485 ± 0.218	0.5 ± 0.229	0.511 ± 0.221

Table 2 Symmetry of regular primary movements as a function of start-end target pair and perturbation type

Subject	Start-end target pair	No perturbation	Near perturbation	Far perturbation
L.	45°	0.008 ± 0.086	–0.008 ± 0.086	0.011 ± 0.0854
	90°	0.005 ± 0.108	–0.056 ± 0.092	0.033 ± 0.081
V.	45°	–0.040 ± 0.092	–0.015 ± 0.098	–0.036 ± 0.117
	90°	–0.018 ± 0.014	–0.063 ± 0.144	0.073 ± 0

In summary, we found evidence for very modest effects of visual perturbations on the kinematics of the primary movement in one of the two monkeys. Next, we examine the effect of visual perturbation on the corrective submovements.

Effects of perturbation on the first corrective submovement

In the following we examine the effect of the perturbation on the occurrence and the type of the first corrective submovement that follows the primary movement. We restrict our analysis to the first correction since later corrections are smaller in extent and peak velocity, and therefore their separation and analysis is more sensitive to noise. Based on the occurrence and type of the first correction we divide individual trials into the following three categories: (1) No corrective submovement, i.e., the trial contained one regular primary movement with no subsequent corrections, (2) Overlapping submovement, i.e., the first correction was overlapping the primary movement, and (3) Delayed submovement, i.e., the first correction did not overlap the primary movement.

Figure 4 shows the rate of occurrence of these categories for each perturbation type in the 45° and 90° trials for monkey L. and V. The percentage values are with respect to the same perturbation condition (no, near and far perturbation) and the same trial extent (45°, 90°). The visual perturbation had a significant effect on the type of the first corrective submovement both for the 45° and 90° trials in both monkeys. (monkey L. 45° trials, $X^2_{(4,N=4808)} = 607, P < 0.05$; 90° trials, $X^2_{(4,N=2364)} = 129, P < 0.05$. monkey V. 45° trials, $X^2_{(4,N=1787)} = 21.2, P < 0.05$; 90° trials, $X^2_{(4,N=854)} = 31.3, P < 0.05$). The most prominent effect of the perturbation on the correction type is the increased number of 'no correction' trials and decreased number of 'overlapping correction' trials under the near perturbation condition (and see also Fig. 2). For the 45° trials there was also a significant increased number of 'delayed corrections' under the far perturbation condition. The reason that fewer corrections are required under the near perturbation condition and more corrections are required under the far perturbation condition is that the primary movements tend to undershoot the target (see Table 1, Fishbach et al. 2005). This phenomenon is illustrated in more detail in Fig. 5 for the 45° trials performed by monkey L. The figure plots the histogram of the end position of the primary movement relative to the target center for each perturbation condition and correction type. The first row ('no perturbation' condition) clearly demonstrates that the primary movement tends to undershoot the target (blue line). In almost all the trials in which the primary movement ended outside of the target limits, the primary movement was followed by a correction. Far perturbations (third row) bring the perturbed target (red line) away from the moving cursor and more trials need to be corrected, mainly by delayed submovements. Conversely, near perturbations (second row) bring the perturbed target closer to the moving cursor and because of the primary undershoot fewer trials need

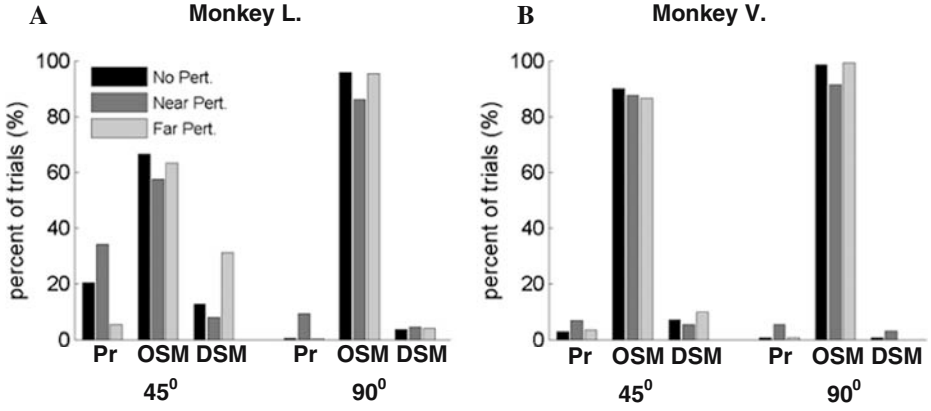

Fig. 4 Rate of occurrence of trials with no corrections (Pr), overlapping submovements (OSM) and delayed submovements (DSM) per perturbation condition and trial extent for monkey L. (**a**) and monkey V. (**b**). Notice the increased number of 'no correction' trials and decreased number of 'overlapping correction' trials under the near perturbation condition

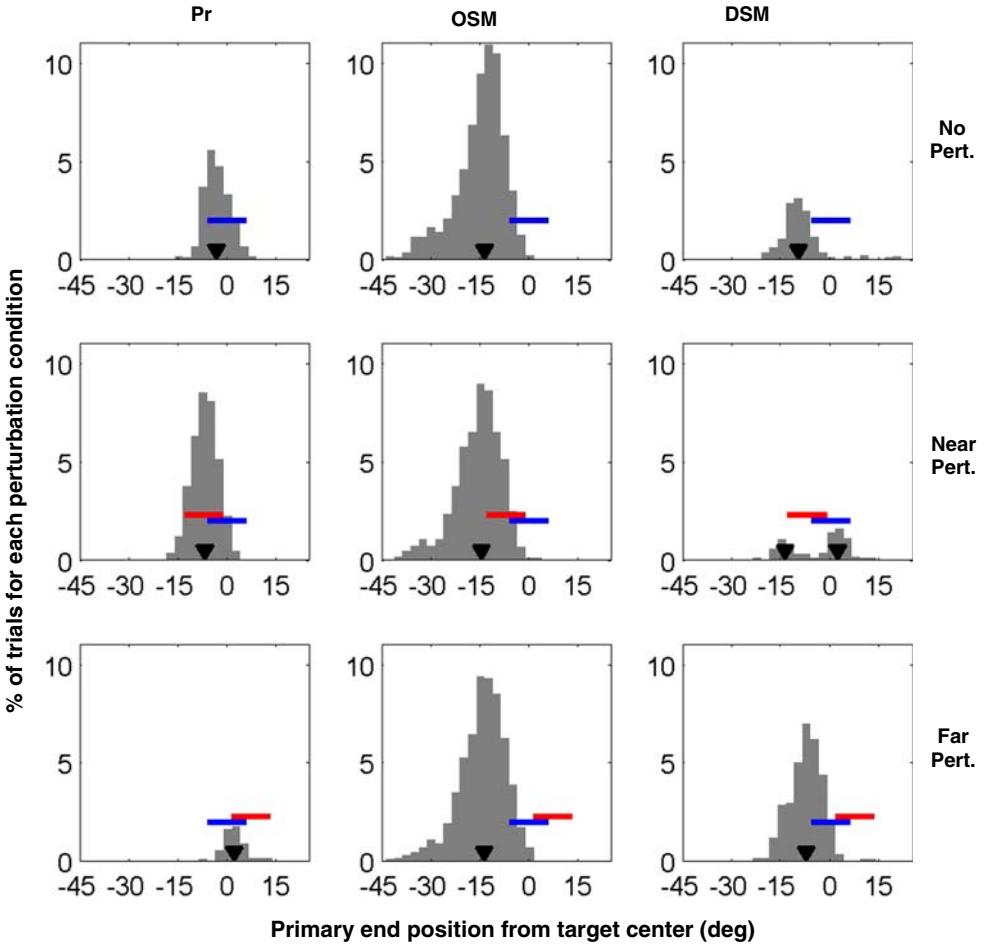

Fig. 5 Distribution of the primary's end position relative to target center per perturbation condition plotted separately for each correction type. The *blue* and the *red lines* represent the target's location before and after the perturbation, respectively. The *inverted black triangle* marks the median of the distribution. The primary movements undershoot the target on average. Primary movements that end up close to the target tend to be corrected by delayed submovements where primary movements that would have ended further from the target tend to be corrected with overlapping submovements. Overshoots (second row, *right panel*) are corrected using delayed submovements

subsequent corrections. Note that under near perturbation, delayed submovements correct both primary movements that slightly undershoot the perturbed target and primary movements that overshoot the perturbed target. Figure 5 also demonstrates that the type of correction (OSM vs. DSM) depends on the end position of the primary movement relative to the target center. This phenomenon will be discussed later in the manuscript. Notably, not only the primary movement tended to undershoot the target, but the overall movement as well tended to be hypometric, with movements falling short of the target's center by 1.15 ± 3.35° for monkey L. and by 0.69 ± 3.37° for monkey V.

Interestingly, many overlapping corrections were unnecessarily used under the near perturbation condition. Figure 5, center panel, demonstrates that for many OSM trials the end-position of the primary movement alone would have brought the cursor within the boundaries of the perturbed target. In contrast, delayed submovements were rarely used unnecessarily under similar conditions. Since by definition delayed submovements tend to be initiated later than overlapping submovements these data suggest that in many cases the overlapping submovements were initiated before the visual information regarding the perturbation was integrated into the control system. In order to test this hypothesis, trials were sorted according to the duration of their primary movements and divided into equal sized groups. For each group we calculated the percentage of trials that included OSMs under the near-perturbation and no-perturbation conditions. Assuming a visual feedback delay, Δ_{visual}, of some fixed value, then for trials with primary movement duration that is shorter than Δ_{visual} the occurrence of an overlapping submovement should be independent of the perturbation type. However, for a group of trials with primary movement durations that exceed Δ_{visual}, fewer trials are expected to have overlapping submovement because of the primary movement's tendency to undershoot. Therefore, by comparing the percentage of OSM trials between the near-perturbation and no-perturbation conditions one can estimate the value of Δ_{visual}. Figure 6a,b plot the percentage of OSM trials for the no-perturbation and near-perturbation conditions for monkey L. and V. The OSM percentage is plotted as a function of the mean duration of the primary

movements in each group of trials. For both monkeys the number of OSM trials under the near perturbation condition decreases compared to the no perturbation condition as the duration of the primary movement increases. The significance of the perturbation effect on the OSM occurrence was calculated using a chi-square test. The *X*-symbols in panels c and d plot the significance level per each group of trials. The three-point smoothed significance as a function of the primary duration is shown by the black solid curve for illustrative purposes. The perturbed target had a significant effect on the overlapping corrections after 192 ms for monkey L. and 230 ms for monkey V., as marked by the vertical dashed lines in panel C and D. These results were not sensitive to the details of the analysis; analyzing 45° and 90° trails separately or changing the size of the trials group had a minor effect on the results.

First OSM initiation time

Examining the effect of perturbation on the initiation time of the first correction relative to movement onset (Table 3) shows that far perturbations did not have an effect on the correction latency of OSMs in monkey L. (45° $t_{1972} = 0.83$, $P > 0.05$; 90° $t_{1499} = 1.1$, $P > 0.05$) and had a significant effect in monkey V. only on 90° trials (45° $t_{1015} = 1.61$, $P > 0.05$; 90° $t_{541} = 2.37$, $P < 0.05$).

Near perturbation had no significant effect on the OSM latency in monkey V. (45° $t_{1037} = 1.76$, $P > 0.05$; 90°, $t_{552} = 0.6$, $P > 0.05$). In monkey L. the OSM latency under near perturbation was shorter than OSM latency under no perturbation condition (45° $t_{1894} = 4.33$, $P < 0.05$; 90° $t_{1444} = 2.41$, $P < 0.05$). However, overlapping submovements are not initiated sooner under near perturbation but rather fewer OSMs are initiated after the visual information became available to the control system (Δ_{visual}) thus reducing the average OSM latency for near perturbation. Indeed, when OSM with latencies longer than 190 ms were excluded from the analysis, there was no significant effect of the near perturbation on the correction initiation time (45°, no pert. 138 ± 34.9 ms, near pert. 137 ± 35.2 ms, $t_{1460} = 0.95$, $P > 0.05$; 90°, no pert. 132 ± 31 ms, near pert. 131 ± 30.7 ms, $t_{1223} = 2.41$, $P > 0.05$).

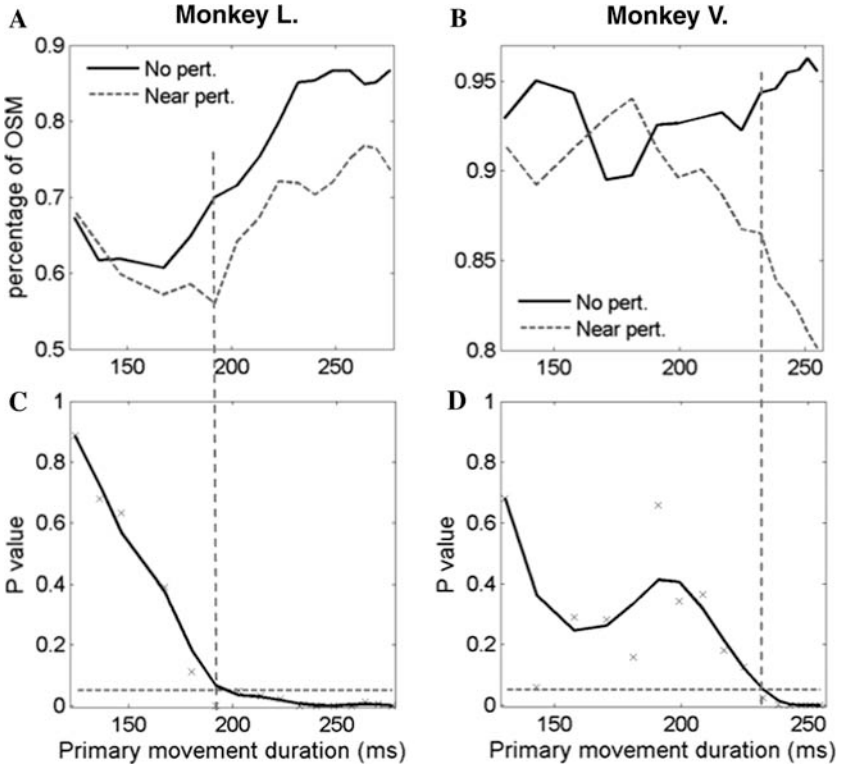

Fig. 6 Analysis of the earliest time the visual perturbation had an effect on the occurrence of corrections. Trials were sorted according to the primary movement duration and divided into equal sized groups ($N = 900$ for monkey L. and $N = 400$ for monkey V.) with overlap such that the duration of the longest primary movements in successive groups were 10 ms apart. **a**,**b** Percentage of OSM trials in each group for the no-perturbation and near-perturbation conditions for monkey L. and V. The OSM percentage is plotted as a function of the mean duration of the primary movements in each group of trials. **c**,**d** Significance of the perturbation effect on the OSM occurrence as calculated using a chi-square test. *X*-marks show the significance level for each group of trials. A three-point smoothing curve of the significance (*solid curve*) is shown for illustrative purposes

Table 3 Latency of first corrective submovement

Subject	First correction type	Trial extent	No perturbation	Near perturbation	Far perturbation
L.	OSM (re. primary onset)	45°	159 ± 48.4	150 ± 43.2	158 ± 51.6
		90°	147 ± 45.3	142 ± 41.7	150 ± 46.7
	DSM (re. primary offset)	45°	103 ± 78.1	169 ± 123	106 ± 71.7
		90°	96 ± 88.9	173 ± 125	88.8 ± 96.4
V.	OSM (re. primary onset)	45°	116 ± 35.7	112 ± 33.2	113 ± 35.6
		90°	117 ± 43.2	115 ± 41.3	127 ± 50.4
	DSM (re. primary offset)	45°	86 ± 60.4	137 ± 91.6	84.5 ± 66.4
		90°	22 ± 8.49	164 ± 63.9	–

First DSM initiation time

The initiation time of delayed submovements was calculated relative to the end time of the primary movement and not with respect to movement onset, to eliminate possible effects of the primary movement duration. Far perturbation had no significant effect on the latency of delayed submovements for either monkey, and for both 45° and 90° trials (Table 3). DSM latencies under near perturbation were significantly longer than under the no perturbation condition (Monkey L.: 45° $t_{311} = 5.78$, $P < 0.05$; 90° $t_{63} = 2.8$, $P < 0.05$; Monkey V.: 45° $t_{66} = 2.76$, $P < 0.05$; 90° $t_8 = 3$, $P < 0.05$).

First OSM normalized amplitude

For the purpose of analyzing the perturbation effect on the normalized amplitude of the first OSM, the normalized amplitude was calculated as the ratio between the OSM extent and the distance to the *original* target center at the time of OSM initiation. The normalized amplitude of the first OSM was smaller under the near perturbation condition than under no perturbation condition (Table 4). For monkey L. this effect was statistically significant for both the 45° and 90° trials ($t_{1894} = 9.64$, $P < 0.05$ and $t_{1444} = 15.8$, $P < 0.05$, respectively). For monkey V. the effect was statistically significant for the 90° trials ($t_{552} = 5.1$, $P < 0.05$) but not for the 45° trials ($t_{1027} = 0.9$, $P > 0.05$). Under the far perturbation condition the normalized amplitude of the first OSM was higher than under the no perturbation condition but only for the 90° trials ($t_{1499} = 3.6$, $P < 0.05$ for monkey L. and $t_{541} = 2.5$, $P < 0.05$ for monkey V.).

In order to examine whether the effect of the perturbation on the OSM normalized amplitude depends on the latency of the OSM we divided the trials to equal size groups of trials of ascending OSM latency. The average OSM amplitude for each group, calculated separately for each perturbation condition, is plotted in Fig. 7. Panel a and c plot the average OSM amplitude for 45° trials performed by monkey L. and for 90° trials performed by monkey V., respectively. The significance of the amplitude difference between near and no perturbations and between far and no perturbation was calculated for each group using a *t* test. The significance levels for the near-no comparison (blue) and the far-no comparison (red) are plotted in panels b and d using same conventions as Fig. 6. For both monkeys the effect of the near perturbation on the OSM amplitude is apparent relatively early (110 ms for monkey L. 45° trials and 90 ms for monkey V. 90° trials). Since the influence of the visual perturbation on the initiation of an OSM is evident much later (at about 200 ms, see Fig. 6) this finding suggests that at least part of the OSM amplitude change is due to a continuous update to the ongoing OSM.

To evaluate the amount of continuous update to the OSM amplitude we analyzed the normalized amplitude of overlapping submovements with latencies shorter than 150 ms and with stop times of at

Table 4 Normalized amplitude of first corrective submovement

Subject	First correction type	Trial extent	No perturbation	Near perturbation	Far perturbation
L.	OSM	45°	0.759 ± 0.339	0.619 ± 0.281	0.771 ± 0.409
		90°	0.715 ± 0.259	0.52 ± 0.199	0.776 ± 0.375
	DSM	45°	0.875 ± 0.383	0.655 ± 0.41	1.21 ± 0.451
		90°	0.83 ± 0.317	0.391 ± 0.214	1.21 ± 0.528
V.	OSM	45°	0.673 ± 0.303	0.657 ± 0.291	0.636 ± 0.297
		90°	0.592 ± 0.234	0.503 ± 0.17	0.657 ± 0.374
	DSM	45°	0.763 ± 0.389	0.69 ± 0.488	1.42 ± 0.373
		90°	0.843 ± 0.274	0.271 ± 0.0784	–

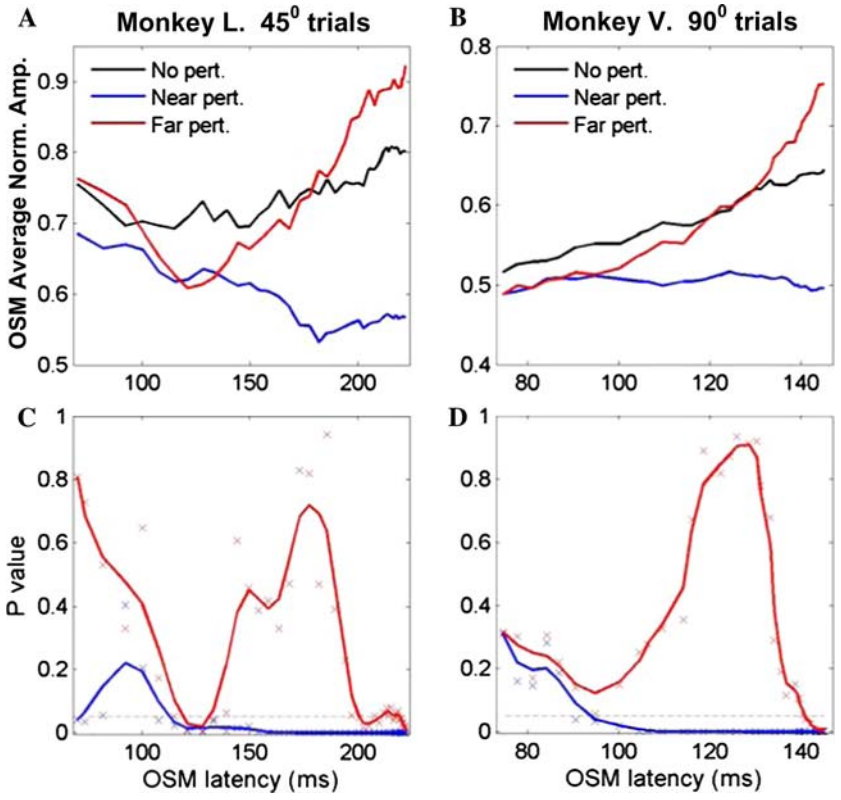

Fig. 7 Effect of perturbation on OSM normalized amplitude as a function of the OSM latency. OSM trials were sorted according to OSM latency and divided to equal size groups ($N = 500$) with overlap such that the latest OSM latency in successive groups were 5 ms apart. Mean OSM normalized amplitude of each group per perturbation condition is plotted as a function of the mean OSM latency of the group for 45° trials of monkey L. (**a**) and 90° trials of monkey V. (**b**). **c**,**d** Significance of the perturbation effect on the OSM normalized amplitude. Conventions are as in Fig. 6

least 220 ms after perturbation onset. These submovements were initiated before the visual perturbation affected their planning but ended after the perturbation information became available. For monkey L. the average normalized amplitude under the near perturbation condition were 11 and 18% smaller than under the no perturbation condition for the 45° and 90° trials respectively. For monkey V. the average normalized amplitude change was 12% for the 90° trials. These findings are consistent with the relatively small early updates observed during the early stages of reaching movements in the monkey (Fishbach et al. 2005), and with larger early updates observe in human reaching movements (Messier and Kalaska 1999; Krakauer et al. 2002) and force pulses (Gordon and Ghez 1987).

Interestingly, the effect of near and far perturbation on OSM amplitude seems to be similar for OSM that were initiated less than 110 ms after movement (and perturbation) onset. The OSM amplitude started to increase, as expected, only for OSMs with latencies longer than 120 ms. Similar results were obtained for 90° trials performed by monkey L. For the 45° trials performed by monkey V. the effect of the near and far perturbation on the OSM normalized amplitude was significant only for OSM with latencies longer than 140 ms.

First DSM normalized amplitude

Table 4 shows that the DSM amplitude was very much affected by the visual perturbation. DSM amplitude was significantly lower under the near perturbation than under the no perturbation condition for both monkeys and both trials extents. Correspondingly, DSM amplitude under the far perturbation was significantly higher than under the no perturbation condition. This finding is not surprising given that delayed submovements are initiated, on average, later than overlapping submovements and therefore are more likely to take into account the new target's location.

Effect of primary normalized amplitude on the first correction type and latency

As shown in Fig. 5 the primary movement end-position relative to the target center had an effect on the type of the ensuing correction (OSM vs. DSM). When no perturbation was present the ensuing corrective submovement tended to be delayed when the primary endpoint was closer to the target (L. 45°, –15.1 ± 7.53 vs. –8.7 ± 7.31; 90° –37.5 ± 14.1 vs. –18.6 ± 11.9; monkey V. 45° –17.8 ± 7.79 vs. –8.47 ± 6.88, 90° only two DSM trials; all comparison were significant using wilcoxon test, $P < 0.05$). We interpret overlapping

submovements as early corrections that do not qualitatively differ from delayed submovements. Thus, we interpret the effect of the primary's normalized amplitude on the correction type as an effect on the correction timing. If this interpretation is correct we should expect that the primary's normalized amplitude will also affect the latency of overlapping submovements.

Figure 8a,b show that for both monkeys and both trials extents the OSM latency is positively correlated with the normalized amplitude of the primary movement; the higher the normalized amplitude (and thus smaller the expected error of the primary movement) the more delayed is the overlapping correction. Note that the correction is initiated well before the primary movement ends, which suggests that a prediction of the primary's endpoint is used to determine whether a correction is needed. Such a prediction may be based on an efferent copy of the neural signal and a proprioceptive feedback (most of the OSMs are initiated before visual feedback is available). Similar correlation also exists between the latency of later OSMs and the normalized amplitude of the preceding submovement. Figure 8c,d demonstrate the correlation between the latency of the second OSM and the normalized amplitude of the first OSM.

To test whether the correlation between the OSM latency and the primary normalized amplitude is an epiphenomenon that is caused by a relationship between the OSM latency and other kinematic variables we performed a stepwise linear regression between the OSM latency and several kinematic properties of the primary movement. Those included the primary extent, duration, peak velocity, time of peak velocity and the primary end position relative to the target. The primary normalized amplitude was the variable that accounted for the most of the variance of the OSM latency (45.7% in monkey L. and 43.3% in monkey V.). The variable that accounted for most of the residual variance (18% in monkey L. and 21.1% in monkey V.) was the time of peak velocity (with a positive regression coefficient). The rest of the variables did not have a significant contribution to the residual variance.

A possible explanation for the correlation between the latency of a corrective submovement and the normalized amplitude of the preceding submovement is that smaller amplitude of the preceding submovement

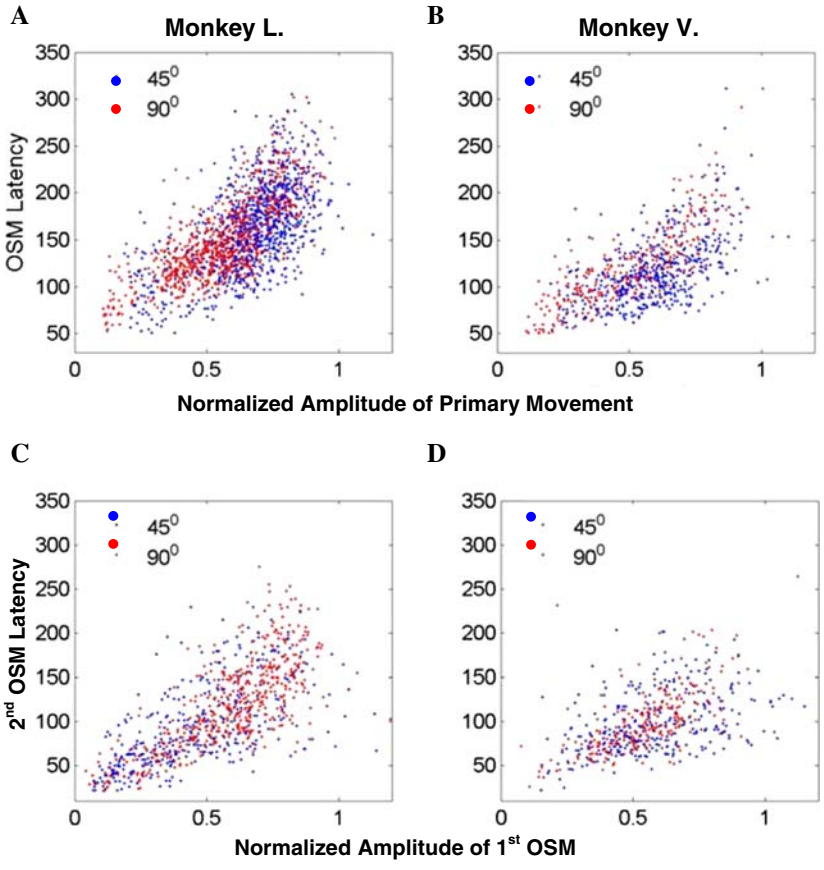

Fig. 8 **a**,**b** OSM latency as a function of the primary normalized amplitude (r^2 = 0.457 for monkey L. and r^2 = 0.433 for monkey V.) (**c**) and (**d**). The same relationship also exists between the second OSM latency and the first OSM normalized amplitude (r^2 = 0.489 for monkey L. and r^2 = 0.134 for monkey V)

will cause a larger correction with higher acceleration. Larger correction may tend to have shorter initiation time resulting from peripheral neuromuscular processes (Ghez and Vicario 1978). However, two observations render this explanation incomplete. First, the range of latencies observed in our data spans over more than 200 ms (Fig. 8), which is much larger then the latency differences observed by Ghez and coworkers. Second, in both monkeys, the correlation between the normalized amplitude of the primary movement and the latency of the first OMS is bigger than the correlation between the OSM latency and its amplitude (monkey L. $r = 0.68$ vs. $r = -0.47$; monkey V. $r = 0.66$ vs. $r = -0.36$).

Another possible concern is that the relationship between the OSM latency and the primary normalized amplitude is an artifact that is caused by the specific details of the decomposition algorithm. To rule out this possibility we tested the correlation between two kinematic properties of the original irregular velocity trace, from which the primary movement and the OSM were extracted, which are correlated with the primary normalized amplitude and the OSM latency. For the normalized amplitude calculation we used the extent of the compound movement at the time of the first peak velocity. The latter is correlated with the primary extent since the first peak velocity of the compound velocity trace is a close approximation for the peak velocity of the primary movement. Since the movement primitives tend to be symmetric, the extent of the movement at the time of first peak velocity approximates half the extent of the extracted primary movement. As an analog for the OSM latency we used the time of the second peak or the saddle point of the velocity trace as explained in Fishbach et al. (2005). Since the duration of the overlapping correction varies, this approximation is very noisy. Nevertheless, we found the two kinematic properties of the original velocity trace to be correlated ($r^2 = 0.205$ for monkey L. and $r^2 = 0.303$ for monkey V.) Note that for measuring both kinematic properties we used the time of the first and second peaks of the original velocity trace as an approximation for the time of peak velocity of the primary movement and of the first OSM, respectively. To test the validity of this approximation we created a set of simulated movements, each is a superposition of a couple of movement primitives of Gaussian velocity profile. The duration of each primitive was in the range of 150–250 ms and the inter-primitive interval ranged from 70 to 200 ms. These parameters reflected the typical values in our data set (Fishbach et al. 2005). We found that the average deviation of the peaks in the combined velocity trace from the actual primitive peaks was 1.7 ms with a standard deviation of 6.7 ms.

This finding suggests that the correlation between the primary normalized amplitude and the latency of the first correction can be observed in the original velocity trace and is not an artifact of the decomposition algorithm.

We also tested whether the primary normalized amplitude is correlated with the value of several kinematic variables at the time of OSM initiation, t_{OSM}. The kinematic variables included the velocity of the primary movement at OSM initiation, the extent to go (the total extent of the primary movement minus the extent at the time of OSM initiation) the percentage-extent-to-go, the duration-go-to (remaining duration of the movement) and the percentage-duration-to-go. In both monkeys the percent-extent-to-go, X, was the variable that was most correlated with the normalized amplitude of the primary movement ($r^2 = 0.487$ and $r^2 = 0.364$ for monkey L. and V., respectively). In both monkeys the relationship between the percent extent to go and the primary movement's amplitude was not linear and was better fitted by an exponent of the percent-extent-to-go squared, (see Fig. 9a,b). The correlation coefficients of the regression $\hat{A} = b + ae^{X^2(t_{OSM})}$ were $b = 1.05 \pm 0.02$, $a = -0.33 \pm 0.01$ for monkey L. and $b = 1.04 \pm 0.04$, $a = -0.3 \pm 0.02$ for monkey V.

Similar correlation also exists between the percent-extent-to-go of later OSMs and their normalized amplitude. Figure 9c,d demonstrate the correlation between the percent-extent-to-go of the first OSM (at the time of initiation of the second OSM) and the normalized amplitude of the first OSM. The correlation coefficients for the first OSM were very similar to those for the primary movement ($b = 0.97 \pm 0.04$, $a = -0.28 \pm 0.02$ for monkey L. and $b = 0.89 \pm 0.07$, $a = -0.2 \pm 0.04$ for monkey V)

A model for first correction initiation

In the previous section we have shown that the primary normalized amplitude is best correlated with the exponent of the percent-extent-to-go squared such that the following approximation holds for both monkeys:

$$\frac{1-\hat{A}}{e^{X^2(t_{OSM})}} \cong 0.33.$$

This relationship suggests that an OSM is initiated when the ratio between the expected error and a monotonically decreasing function of movement progression reaches a constant value.

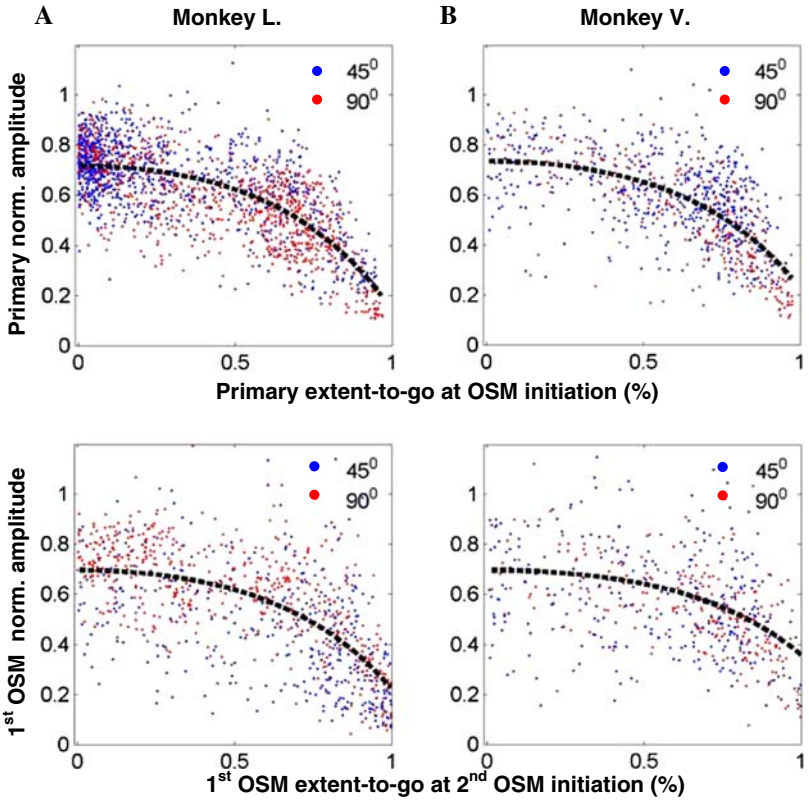

Fig. 9 **a**,**b** Primary normalized amplitude as a function of the primary percent-extent-to-go at the time of OSM initiation. For both monkeys the data was best fit by the exponent of the percent-extent-to-go squared (*dashed curve*) (**c**) and (**d**). The same relationship also exists between the first OSM normalized amplitude and its percent-extent-to-go at the time of the second OSM initiation time

A possible interpretation of this finding is that the denominator of the above fraction is proportional to the variance of the estimated error and that a correction is initiated when the estimated z-score of the error crosses a fixed threshold (Fig. 10a). Figure 10b illustrates schematically how the probability density function (p.d.f.) of the predicted endpoint might change as the movement progresses and how the endpoint's p.d.f. affects the decision for correction initiation. To test this hypothesis we implement a simple abstract model whose principles are based on the above observations. In the model we assume that a correct estimate of the *mean* predicted error (1-$\hat{A}$) is known at movement onset and does not change during the course of the movement. The standard deviation of the predicted error (which changes throughout the movement) is normalized between the range of 0 to k, where k is a free parameter, and is assumed to be:

$$\sigma(t) = k\frac{e^{X^2(t)} - 1}{e^1 - 1}.$$

The correction latency is defined as:

$$L = \min_{0<t\le D}\left\{\frac{1-\hat{A}}{\max\{\sigma(t), \sigma_m\}} \ge T\right\},$$

where T is the z score threshold and σ_m reflects a minimal amount of variance in the estimation of the cursor position at the end of the movement due to a possible combination of internal and external noise. We set σ_m to a value of 0.005 and optimized the two free parameters k and T to maximize the correlation between L and the actual latency of the first overlapping submovement. For that optimization we used a training set that included a third of the unperturbed trials of monkey L. for which the first correction was an overlapping submovement. Figure 11a,b plot the actual OSM latency versus the model latency predictions for monkey L. and V., respectively, using $k = 0.4$ and $T = 1.56$ (the latter corresponds to a confidence level of 0.06). For monkey L. we excluded the training set data. The dashed gray line plots the regression line between the predicted and actual latency. For monkey L. the line's slope was 0.982 ± 0.0587 and the intercept was 76.4 ± 5.45 ms ($r^2 = 0.5$). For monkey V. the slope of the regression line was 0.977 ± 0.068 and the intercept was 54 ± 5.3 ms ($r^2 = 0.56$). The regression's intercept correspond to a delay that may be caused by both afferent and efferent delays.

The results were not sensitive to values of the parameters used but the exact values of k and T were not well restricted by the maximization; the optimum

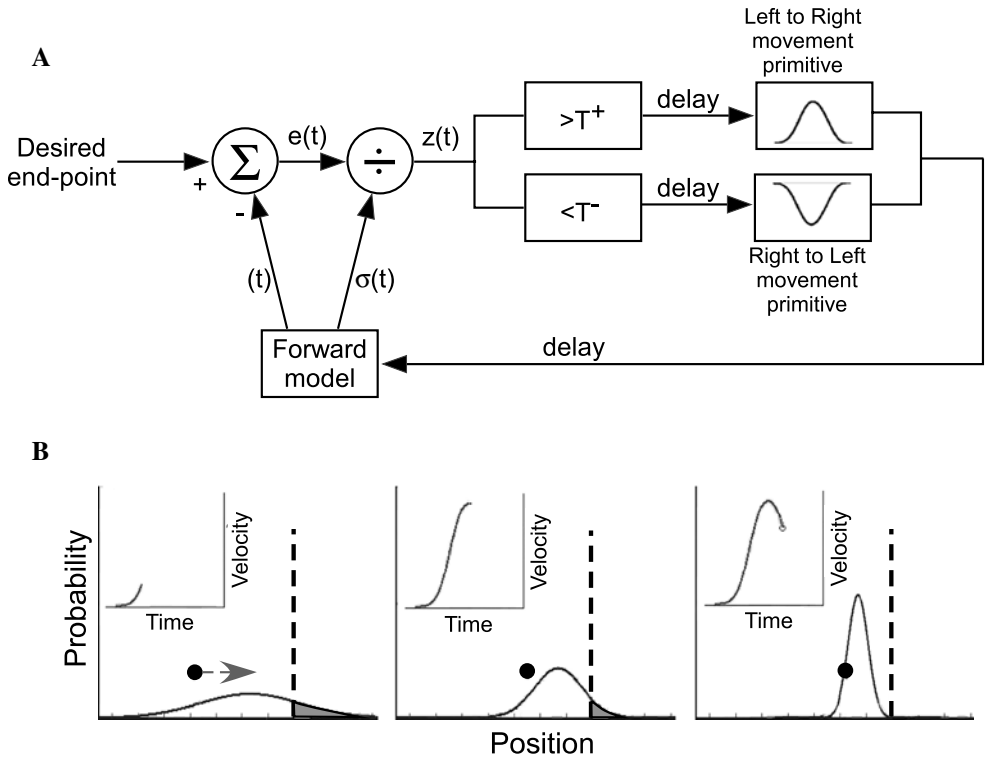

Fig. 10 **a** An abstract model that accounts for the timing of corrections observed in our data. A forward model predicts the endpoint of the ongoing movement. The discrepancy between the desired and predicted endpoints is normalized by the prediction standard deviation. A dead-zone is used to initiate a bell-shaped correction only when the normalized endpoint error exceeds a threshold. **b** A schematic illustration of the predicted endpoint p.d.f. at different moments of the movement. Each panel plots the endpoint p.d.f., the target location (*dashed line*) and the cursor's instantaneous position (*filled circle*). The inner inset of each panel plots the movement velocity as a function of time. The Initial endpoint estimation (*left panel*) suggests undershoot. However the estimation is very noisy and no correction is initiated. As more feedback is available (*middle panel*) the endpoint prediction is less noisy but the tail of the distribution is still too large and no correction is initiated. After more feedback is available and the horizon of the prediction shortens (right panel) the deviation of the endpoint from the target is significant and a correction is initiated

was relatively flat along a curve in the $[k,T]$ plane (not shown), since increasing or decreasing the values of k and T simultaneously near the optimum had a very limited effect on the predicted latency. Different values for σ_m in the range of 0.05–0.0005 were also tested and found to little change the optimization results.

Figure 11c,d plot the distribution of the model's OSM latency relative to the end-time of the primary movement for all the unperturbed trials of monkey L. and V., respectively. For comparing the model's predictions and the end-time of the primary movement we added to the predicted latency the value of the delay as given by the regression intercept. The bars to the right of the vertical dashed line represent the trials for which the model did not predict a correction until the end of the primary movement. Note that the model predicts an overlapping submovement for some of the trials that in practice did not have an overlapping correction, but in these cases the model's latency tends to be relatively close the end-time of the primary movement.

Since the visual perturbations did not change the initiation time of OSMs (See Table 3) the model predicted well the OSM latency of perturbed trials. However, the number of non-OSM trials for which the model predicted an overlapping correction increased under visual perturbations, as expected.

Discussion

We studied the effect of visual perturbation of a target on the kinematics of fast step-tracking movements in the monkey. In particular, we analyzed the effect of the perturbation on the normalized amplitude and timing of primary movements and on the corrective submovements that usually follow them. In general, our data show little evidence for a continuous update process, in agreement with our previous study (Fishbach et al. 2005). There was a very small effect of the visual perturbation on the symmetry of the

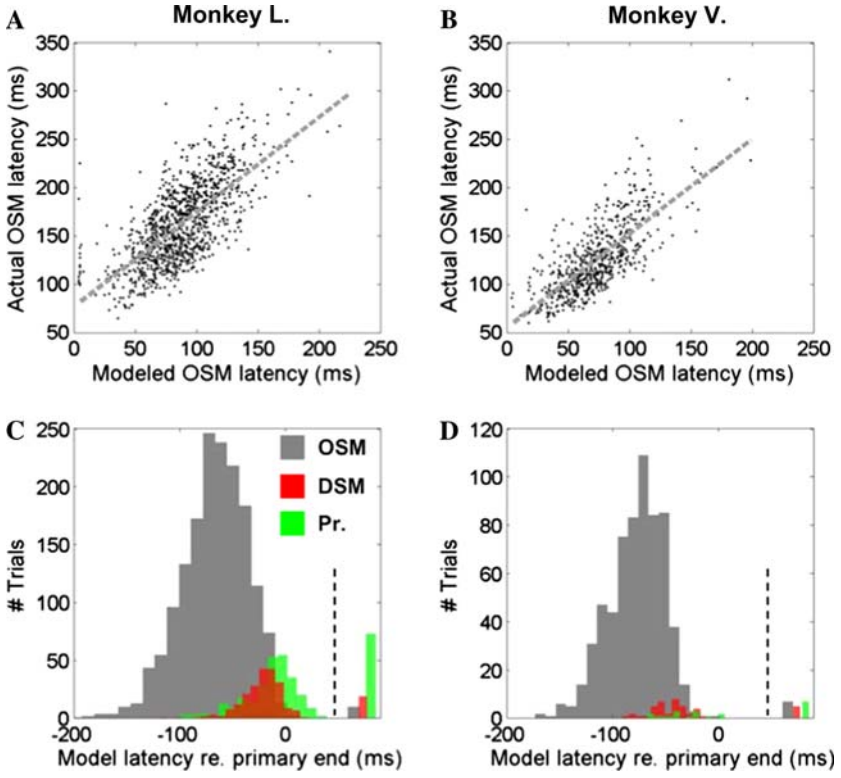

Fig. 11 Actual versus predicted OSM latency for monkey L. (**a**) and V. (**b**). **c**,**d** Distribution of predicted OSM latency relative to the end-time of the primary movement for all unperturbed trials of monkey L. (**a**) and V. (**b**). Data is plotted separately for trials of different actual correction types. *Bars to the right of the vertical dashed line* represent trials with no predicted correction. The model produces overlapping correction for some of the DSM trials but they tend to start near the end of the primary movement

primary movement in one of the two monkeys. A slightly larger contribution of continuous update was found for the first OSMs when it began before visual information became available; the normalized amplitude of the latter was 11–18% smaller under the near perturbation condition than under the no perturbation condition.

Most of the effects of visual perturbation were discrete in nature. Perturbations changed dramatically the number of corrections used to obtain the target. Fewer submovements were used under the near perturbation condition whereas more were used under the far perturbation condition, consistent with the fact that primary movements tended to undershoot the target (see Table 1). However, this undershoot was not provoked by the presence of the perturbation since it was evident even when perturbed trials were not included in the experimental procedure (Fishbach et al. 2005). We conclude that the strategy adopted by the monkeys was to undershoot the target on average and to correct in the direction of the primary movement using discrete corrections, which avoided having to break the movement or change the direction of motion. This strategy was also adopted by human subjects in a similar task (Novak et al. 2000) and is probably used to minimize total movement time under conditions of noise and neural delays (Harris 1995; Kositsky and Barto 2001; Engelbrecht et al. 2003).

OSM latencies reflect a predictive controller with a dead-zone

In most cases, the corrections started before the primary movement ended, which suggests that a prediction of the primary normalized amplitude was available to the control system relatively early in the movement. Although the existence of a forward model (Jordan and Rumelhart 1992) for predicting the movement endpoint may explain the occurrence of corrections before the end of the primary movement, it may not necessarily account for the relationship between the normalized amplitude of the primary movement and the timing of the correction reported here. Sliding variable control (Hanneton et al. 1997), which uses a threshold non-linearity on the predicted error, is not likely to account for such a relationship unless one assumes that the predicted error is always smaller than the threshold at the beginning of the movement and increases monotonically to the true error as the primary movement progresses. This requires that the predicted error be biased and always underestimated, which is unlikely.

We suggest that the relationship between the primary movement's amplitude and the latency of the OSM is mediated by the *variance* of the predicted amplitude. We found for both monkeys that the correction occurred when the ratio between the expected

error (one minus the normalized amplitude) and the exponent of the percent extent to go squared reached a constant value. Since the extent to go is a monotonically decreasing function of time, it is appealing to relate it to a variance measure of the predicted error, which presumably also decreases monotonically as movement progresses. This formulation is especially appealing since it puts the empirical relationship between the OSM latency and the predicted error of the primary movement in the context of statistical decision theory (Berger 1985). We thus suggest that a *decision* to correct is made when the *probability distribution* of the predicted end-point is statistically different from the target's location. Indeed, we show that a simple abstract model that implements these principles can predict quite well the observed OSM latencies. Interestingly, the actual OSM latencies lag the predicted ones by 45–65 ms, which probably reflects feedback delays. Neural mechanisms and models for decisions-making processes that lead to initiation of actions have been suggested (Carpenter and Williams 1995; Glimcher 2003; Cisek and Kalaska 2005). At the core of these models is the concept of gradual accumulation of evidence until a decision threshold is met. Here we suggest that a similar mechanism can be applied not only for the initiation of movements but also for the initiation of discrete online error corrections.

The neural mechanisms that underlie on-line correction of reaching movements are not well understood. Several cortical areas have been implicated in the process of on-line error correction (Desmurget et al. 1999; Tunik et al. 2005), but only when the target is visually perturbed. Other studies have demonstrated that patients with basal-ganglia dysfunctions show deficits in on-line error correction (e.g., Smith et al. 2000; Smith and Shadmehr 2005; Tunik et al. 2004). Recently, Houk et al. (2006) have suggested that the powerful computational features of the cortical loops through the basal ganglia are capable of calculating a normalized error prediction of the current motor program, which leads to the initiation of a correction when this normalized error crosses a threshold, in agreement with the abstract model proposed here. The model of cortico-basal-ganglionic processing calls for neurophysiological studies of the neural mechanisms that are implicated in the corrections of motor commands. Our behavioral studies in non-human primates will facilitate this line of research.

Discrete versus continuous control

The interpretation of kinematic irregularities in reaching movement has been intensely debated. Some authors have attributed kinematic irregularities to the properties of the neuromusculoskeletal system (Plamondon and Alimi 1997). However, previous studies (Novak et al. 2000) used simulations of the musculoskeletal system to show qualitative incompatibilities between irregularities of experimental velocity traces and the irregularities in simulated kinematics. In addition, it has been shown recently that the firing rate of M1 units of monkeys performing a 1D reaching task show irregularities that are correlated with the kinematic irregularities of the velocity trace (Fishbach et al. 2003). Since the behavior lagged the neural activity, this finding suggests that the kinematic irregularities are not due to the properties of the peripheral neuromusculoskeletal system.

Others studies have suggested that a continuous control process can produce kinematic irregularities that do not reflect superposition of discrete movement primitives (Kawato 1992; Shadmehr and Mussa-Ivaldi 1994; Bhushan and Shadmehr 1999; Sternad and Schaal 1999). Indeed, demonstrating that a velocity trace can be represented by a linear superposition of a set of discrete primitives is not sufficient evidence for the existence of these primitives. However, several findings of our current study are difficult to reconcile with a purely continuous controller and strongly support the hypothesis that the kinematic irregularities are due to a superposition of discrete movement primitives.

First, delayed submovements, which start several dozens of milliseconds after the end of the primary movement, are not consistent with a continuous controller unless one assumes that the delayed correction represents a different phase in the movement control. For example, one can assume that the main (primary and irregular primary) movement is not guided by visual feedback whereas the delayed submovement is delayed and slowed down enough to allow visual guidance.

Secondly, we have shown that the latencies of the overlapping submovements are highly variable. If the irregularities (that we interpret as submovements) are produced by a purely continuous controller, the time of the first irregularity should be relatively fixed with a latency that corresponds to the sensorimotor delay (either proprioception or vision). Correspondingly, we would expect that the effect of the visual perturbation on the occurrence of corrections will occur in a relatively narrow time window with a delay that corresponds to the visuomotor delay. This, however, was not the case. The effects of perturbations on the occurrences of corrections spread over a time window of more than 200 ms.

Thirdly, the dependence of the type of correction (OSM vs. DSM) as well as the OSM latency on the primary movement's amplitude reinforces the notion that the only difference between delayed submovements and overlapping submovements is their initiation time relative to movement onset. This suggests that the same discrete mechanism that initiates the discrete delayed corrections also controls the initiation of the overlapping submovements. It is important to note that the correlation between the primary normalized amplitude and the OSM initiation time represents a phenomenon which is not merely kinematic but also context dependent since the OSM latency was better correlated with the *normalized amplitude* of the primary movement than with its *amplitude*.

Our proposed model may bridge between the purely continuous and the purely discrete interpretations of kinematic irregularities in reaching movements. While the feedback and forward components of the model are continuous, the execution component is triggered in a discrete manor using a threshold non-linearity, i.e. when the noisy prediction of the movement endpoint significantly deviates from the desired target.

It is possible that some of the movement update is done in a continuous manner as well. In this study we found little evidence for a continuous update of the movement, which is consistent with the relatively small early updates observed during the early stages of reaching movements in the monkey performing a similar task with no visual perturbation (Fishbach et al. 2005). Other studies have reported a much larger continuous update in human reaching movement (Messier and Kalaska 1999; Krakauer et al. 2002; Desmurget et al. 2005) and force pulses (Gordon and Ghez 1987). It is possible that the differences between these studies and our findings are partly due to the experimental protocol. For example, in most of those studies the subjects were asked to perform a *single uncorrected* movement with relaxed or no time limits on the movement duration. Conversely, in our study and in the studies of Novak and co-workers (Novak et al. 2000) subjects were under strict time constraint and were free to choose how and if to correct their movement. However, more research is needed in order to characterize the conditions under which continuous update is used.

Our model also gives rise to interesting testable predictions regarding the timing of discrete corrections in reaching movements. We predict that under increased sensory noise, either visual or proprioceptive, discrete corrections will tend to initiate later and/or the normalized amplitude of the movement primitives will become smaller. Thus, we predict that under increased sensory noise the movement's velocity profile will become more segmented. Highly segmented velocity profiles were observed in reaching movements of infants (Berthier 1997), in Huntingon's disease (Smith et al. 2000) and in post-stroke patients (Krebs et al. 1999). New understanding of the mechanisms that underlie movement segmentation may shed new light on the development of motor skills and on the etiology of movement abnormalities in humans with neurological disorders.

Acknowledgments This work was supported by grant NS44383 to James Houk.

References

Berger JO (1985) Statistical decision theory and Bayesian analysis. Springer, Berlin Heidelberg New York

Berthier NE (1996) Learning to reach: A mathematical model. Dev Psychol 32:811–823

Berthier NE (1997) Analysis of reaching for stationary and moving objects in the human infant. In: Donahue J, Dorsal VP (eds) Neural network models of complex behavior—biobehavioral foundations. North-Holland, Amsterdam, pp 283–301

Bhushan N, Shadmehr R (1999) Computational nature of human adaptive control during learning of reaching movements in force fields. Biol Cybern 81:39–60

Carpenter RH, Williams ML (1995) Neural computation of log likelihood in control of saccadic eye movements. Nature 377:59–62

Cisek P, Kalaska JF (2005) Neural correlates of reaching decisions in dorsal premotor cortex: specification of multiple direction choices and final selection of action. Neuron 45:801–814

Desmurget M, Epstein CM, Turner RS, Prablanc C, Alexander GE, Grafton ST (1999) Role of the posterior parietal cortex in updating reaching movements to a visual target. Nat Neurosci 2:563–567

Desmurget M, Turner RS, Prablanc C, Russo GS, Alexander GE, Grafton ST (2005) Updating target location at the end of an orienting saccade affects the characteristics of simple point-to-point movements. J Exp Psychol Hum Percept Perform 31:1510–1536

Engelbrecht SE, Berthier NE, O'Sullivan LP (2003) The undershoot bias: learning to act optimally under uncertainty. Psychol Sci 14:257–261

Fishbach A, Roy SA, Bastianen C, Miller LE, Houk JC (2003) Neural correlates of on-line error correction in M1 of behaving macaque monkey. In: Neural control of movement, Santa Barbara, CA

Fishbach A, Roy SA, Bastianen C, Miller LE, Houk JC (2005) Kinematic properties of on-line error corrections in the monkey. Exp Brain Res 164:442–457

Flash T, Henis E (1991) Arm trajectory modifications during reaching towards visual targets. J Cogn Neurosci 3:220–230

Ghez C, Vicario D (1978) The control of rapid limb movement in the cat. I. Response latency. Exp Brain Res 33:173–189

Glimcher PW (2003) The neurobiology of visual-saccadic decision making. Annu Rev Neurosci 26:133–179

Gordon J, Ghez C (1987) Trajectory control in targeted force impulses. III. Compensatory adjustments for initial errors. Exp Brain Res 67:253–269

Hanneton S, Berthoz A, Droulez J, Slotine JJ (1997) Does the brain use sliding variables for the control of movements? Biol Cybern 77:381–393

Harris CM (1995) Does saccadic undershoot minimize saccadic flight-time? A Monte-Carlo study. Vision Res 35:691–701

Houk JC, Fraser D, Fishbach A, Roy SA, Simo LS, Bastianen C, Wald D, Reber PJ (2006) Action selection and refinement in subcortical loops through basal ganglia and cerebellum. Philos Trans Roy Soc B (in press)

Jordan MI, Rumelhart DE (1992) Forward models: supervised learning with a distal teacher. Cogn Sci 16:307–354

Kawato M (1992) Optimization and learning in neural networks for formation and control of coordinated movement. In: Meyer DE, Kornblum S (eds) Attention and performance, vol XIV. MIT, Cambridge, p 821–849

Kositsky M, Barto AG (2001) Emergence of multiple movement units in the presence of noise and feedback delay. In: Dietterich TG, Becker Z, Ghahramani Z (eds) Advances in neural information processing systems, vol 14. MIT, Cambridge

Krakauer JW, Gordon J, Veytsman M, Ghez C (2002) Contributions of planning and updating to accuracy of reaching movements in normals and stroke. In: Society for Neuroscience, vol Program No. 169.4. 2002

Krebs HI, Aisen ML, Volpe BT, Hogan N (1999) Quantization of continuous arm movements in humans with brain injury. Proc Natl Acad Sci USA 96:4645–4649

Lee D, Port NL, Georgopoulos AP (1997) Manual interception of moving targets .2. On-line control of overlapping submovements. Exp Brain Res 116:421–433

Messier J, Kalaska JF (1999) Comparison of variability of initial kinematics and endpoints of reaching movements. Exp Brain Res 125:139–152

Meyer DE, Abrams RA, Kornblum S, Wright CE, Smith JE (1988) Optimality in human motor performance: ideal control of rapid aimed movements. Psychol Rev 95:340–370

Milner TE (1992) A model for the generation of movements requiring endpoint precision. Neuroscience 49:487–496

Milner TE, Ijaz MM (1990) The effect of accuracy constraints on three-dimensional movement kinematics. Neuroscience 35:365–374

Morasso P, Mussa Ivaldi FA (1982) Trajectory formation and handwriting: a computational model. Biol Cybern 45:131–142

Novak KE, Miller LE, Houk JC (2000) Kinematic properties of rapid hand movements in a knob turning task. Exp Brain Res 132:419–433

Novak KE, Miller LE, Houk JC (2002) The use of overlapping submovements in the control of rapid hand movements. Exp Brain Res 144:351–364

Plamondon R, Alimi AM (1997) Speed/accuracy trade-offs in target-directed movements. Behav Brain Sci 20:279–303; discussion 303–249

Pratt J, Chasteen AL, Abrams RA (1994) Rapid aimed limb movements—age-differences and practice effects in component submovements. Psychol Aging 9:325–334

Saunders JA, Knill DC (2003) Humans use continuous visual feedback from the hand to control fast reaching movements. Exp Brain Res 152:341–352

Shadmehr R, Mussa-Ivaldi FA (1994) Adaptive representation of dynamics during learning of a motor task. J Neurosci 14:3208–3224

Smith MA, Brandt J, Shadmehr R (2000) Motor disorder in Huntington's disease begins as a dysfunction in error feedback control. Nature 403:544–549

Smith MA, Shadmehr R (2005) Intact ability to learn internal models of arm dynamics in Huntington's disease but not cerebellar degeneration. J Neurophysiol 93(5):2809–2821

Sternad D, Schaal S (1999) Segmentation of endpoint trajectories does not imply segmented control. Exp Brain Res 124:118–136

Tunik E, Adamovich SV, Poizner H, Feldman AG (2004) Deficits in rapid adjustments of movements according to task constraints in Parkinson's disease. Mov Disord 19:897–906

Tunik E, Frey SH, Grafton ST (2005) Virtual lesions of the anterior intraparietal area disrupt goal-dependent on-line adjustments of grasp. Nat Neurosci 8:505–511

Woodworth RS (1899) The accuracy of voluntary movement. Psychological Review 3:1–114